Research Paper

# Study on the Mechanism of Yixin Fumai Granules in Improving Fibrosis of Sinoatrial Node in D-Galactose-Induced Senescence Mice Based on Network Pharmacology

LIANZI JIN* AND PING HOU[1]

Department of Traditional Chinese Medicine, Liaoning University of Traditional Chinese Medicine, [1]Department of Cardiology, Affiliated Hospital of Liaoning University of Traditional Chinese Medicine, Shenyang, Liaoning Province 110000, China



**The research utilized network pharmacology to explore how Yixin Fumai granules mitigate sinoatrial node fibrosis caused by D-galactose in older mice by altering inflammatory reactions. Effective ingredients and targets of Yixin Fumai granules (including ginsenoside, ophiopogonin, schisandrin, astragaloside, danshensu, and ligustilide) were screened from traditional Chinese medicine systems pharmacology and BATMAN-traditional Chinese medicine databases. Targeted diseases were pinpointed using GeneCards, Online Mendelian Inheritance in Man, and Disgenet databases. By employing Cytoscape 3.7.2 software, a network targeting drug-effective ingredients-targets was created, accompanied by a protein-protein interaction network formed *via* the Search Tool for the Retrieval of Interacting Genes databases. To forecast the fundamental processes, analyses of Gene Ontology functional enrichment and Kyoto Encyclopedia of Genes and Genomes pathway enrichment were conducted utilizing the R language. The expression levels of the Nucleotide oligomerization domain-like receptor protein 3, caspase-1, gasdermin D, interleukin-1 beta, and interleukin-18 genes were assessed through reverse transcription polymerase chain reaction. A total of 127 components were identified, with major components including quercetin, beta-sitosterol, kaempferol, naringenin, ginsenoside Rb1, and beta-eudesmol. There were 129 therapeutic targets identified, including key targets such as tumor necrosis factor, protein kinase B serine/threonine kinase 1, interleukin-6, tumor protein P53, interleukin-1 beta, and vascular endothelial growth factor A. The experimental findings revealed that the Yixin Fumai granules group mice, in contrast to the model group, showed enhanced mental health, a standard diet, notably better coat color, and zero fatalities. The echocardiographic results showed a rise in ejection fraction and fractional shortening, a faster heart rate, a reduction in left ventricular internal diameter end systole and left ventricular internal diameter end diastole, and an increase in left ventricular posterior wall end systole and left ventricular posterior wall end diastole in the Yixin Fumai granules group relative to the model group. This study preliminarily elucidated the active ingredients, targets, and pathways through which Yixin Fumai granules treat sick sinus syndrome using network pharmacology and further validated its mechanism through experimental verification. These findings provide new evidence and research directions for treating sick sinus syndrome induced by aging.**

**Key words: Yixin Fumai granules, network pharmacology, sick sinus syndrome, bradycardia, fatigue, arrhythmia**

Aging increases the incidence of chronic arrhythmias, with Sick Sinus Syndrome (SSS) being the most prevalent type characterized by dysfunction in the sinoatrial node's pacemaker or conduction function, resulting in bradycardia. Decreased heart rate can lead to inadequate perfusion of organs such as the brain, heart, and kidneys, manifesting symptoms such as palpitations, fatigue, and dizziness, with severe

***Address for correspondence**
E-mail: jjww915@126.com



**Accepted 14 August 2024**
**Revised 22 April 2024**
**Received 05 June 2023**
**Indian J Pharm Sci 2024;86(4):1535-1546**

cases potentially causing syncope or sudden death. Currently, the most effective treatment involves implanting a pacemaker; however, its usage is significantly limited due to technical, economic, and procedural factors. Western medication, with its substantial side effects[1], is unsuitable for long-term oral administration in SSS treatment. Traditional Chinese Medicine (TCM) requires time-consuming preparations, posing challenges in patient compliance. Thus, there is a valuable focus on developing clinically effective and user-friendly Chinese patent medicine for this condition.

## MATERIALS AND METHODS

### Selection of active ingredients and targets of Yixin Fumai (YXFMs) granules:

The TCM Systems Pharmacology (TCMSP) database was utilized to screen for active ingredients such as *Panax ginseng*, *Schisandra chinensis*, *Astragalus membranaceus*, *Salvia miltiorrhiza,* and Chuanxiong, setting the criteria for Oral Bioavailability (OB) to be 30 % or higher and Drug-Likeness (DL) to be 0.18 or more[2]. *Ophiopogon japonicus* (*O. japonicus*) was evaluated using the BATMAN-TCM database, achieving a score of 15 or higher[3]. The UniProt database was utilized to annotate target genes, obtaining their corresponding full protein names and standardized abbreviations, which were then converted to gene names for further analysis.

### Selection of disease targets:

By employing the terms SSS as key terms, specific disease targets were pinpointed using the Genecards, Online Mendelian Inheritance in Man (OMIM), and DisGeNET databases. Targets associated with SSS were consolidated by merging data from these three databases and removing duplicates.

### Construction of drug-ingredient-target network:

The active ingredient targets of YXFMs and disease targets of SSS were imported into the Venny analysis platform to obtain intersecting targets. Based on common targets, the principal active ingredients of YXFMs were identified. Through the application of Cytoscape 3.7.2 software, a network model called drug-ingredient-target was created, featuring nodes that represent various drugs, components, and targets, and edges depicting their interrelations.

### Construction of Protein-Protein Interaction (PPI) network:

Targets that intersected were fed into the Search Tool for the Retrieval of Interacting Genes (STRING) platform[4], identifying *Homo sapiens* as the living organism, establishing an initial interaction score of 0.4, and discarding isolated nodes, to develop the PPI network of YXFMs targeting SSS. The PPI network underwent topological analysis using Cytoscape 3.7.2's NetworkAnalyzer to pinpoint crucial targets, focusing on degrees, betweenness centrality, and closeness centrality exceeding the mean values.

### Gene enrichment analysis:

R software and the org.Hs.eg.db backend database were used to obtain gene IDs of potential target genes. Bioconductor's DOSE, clusterProfiler, and path view tools were utilized for performing Gene Ontology (GO) functional enrichment analysis, encompassing areas such as the study of Biological Process (BP), Cellular Component (CC), Molecular Function (MF), and examining the enhancement of the Kyoto Encyclopedia of Genes and Genomes (KEGG) pathway. The study shed light on crucial biological mechanisms and routes linked to possible targets of action.

### Experimental animals:

Liaoning Changsheng Biotechnology Co. Ltd., provided 30 Specific Pathogen Free (SPF)-grade male C57BL/6 mice, which were licensed under the experimental license (No:SCXK2020-0001). The weight of the mice ranged from (23-25) g, and they were aged between 6 w and 8 w. The subjects were accommodated in SPF-standard experimental animal chambers, kept under regulated conditions; a temperature between 18°-25°, humidity levels of 40 %-60 %, and a light intensity ranging from 150-200 lux, with a cycle of 12 h of light and darkness. SLK standard di was used to nourish the mice ET, with unrestricted access to water. Every aspect of animal care and experimental method adhered rigorously to the ethical standards and protocols sanctioned by our Institution's Animal Experiment Ethics Committee.

### Main drugs and reagents:

YXFMs are a commercially available TCM granule formula for treating arrhythmias (National Drug

Approval No: Z21021261). Interleukin-1 Beta (IL-1β) assay kit (NM_008361.4), IL-18 assay kit (NM_008360.2), Gasdermin D (GSDMD) assay kit (NM_026960.4), Nucleotide Oligomerization Domain (NOD)-Like Receptor Protein 3 (NLRP3) assay kit (NM_001359638.1), Caspase 3 (CASP3) assay kit (NM_009807.2), and Polymerase Chain Reaction (PCR) primers were purchased from Wuhan Suvil Technologies Co. Ltd. The TRIzol® reagent Ribonucleic Acid (RNA) extraction kit (G3013) was acquired from Wuhan Suvil Technologies Co. Ltd.

**Main instruments:**

Hematoxylin and Eosin (H&E) staining solution, modified Masson's trichrome staining solution (Solaibao, China); VEVO2100 animal ultrasound imaging system (Visualsonics, United States of America (USA)); four-channel multi-lead physiological acquisition analysis system (AD Instruments, Australia); paraffin embedding machine (Model: EG1150, Leica, Germany); PCR machine (ETC811, Beijing Dongsheng Innovation Biotechnology Co. Ltd.,); microscope (Nikon Eclipse Ci-L); three-dimensional cryogenic grinder and an instrument for quantitative fluorescence PCR (Bio-rad CFX Connect).

**Model establishment and group administration:**

Following a week-long acclimatization phase, 30 male C57BL/6 mice with SPF-grade were arbitrarily split into three categories; the control, model, and YXFMs groups, allocating 10 mice to each. Mice in the model group and YXFMs group received subcutaneous injections of D-galactose at 200 mg/kg/d at 10 am. daily for 8 w. At identical intervals, the control group mice were administered equal amounts of saline injections. Commencing from the 2nd d after the model, the YXFMs group of mice were given YXFMs orally at a dosage of 1 g/kg/d over a span of 28 d, whereas the other groups were given similar amounts of distilled water orally for the same duration. Following a period of 28 d, electrocardiograms were conducted to evaluate the heart rate and the R-R intervals among the mice in each group. Additionally, heart tissues were collected following a cervical dislocation.

**Condition monitoring:**

During the experiment, the mice's behavioral states, fur color changes, body weights, etc., were observed to assess survival rates.

**Echocardiographic examination:**

At the conclusion of the 8 w therapy phase, echocardiographic tests were conducted. Post-anesthesia, the chest region underwent depilation and was readied for cardiac ultrasound imaging *via* a specialized imaging system. Averaging data from three successive heart cycles helped ascertain the Left Ventricular Internal Dimension in diastole (LVIDd), Left Ventricular Internal Dimension in systole (LVIDs), End-Diastolic Volume (EDV), and the thickness of the Interventricular Septum at end-systole (IVSs). Measurements in every mouse group End-Systolic Volume (ESV), Stroke Volume (SV), Ejection Fraction (EF), and Fractional Shortening (FS).

**Cardiac histopathological observation:**

The sinoatrial node of mice was fixed in 4 % paraformaldehyde. After adequate fixation, the tissue underwent trimming, dehydration, embedding, sectioning, staining, and cover slipping for subsequent pathological staining analysis.

**H&E staining:** Post-scanning, H&E staining was conducted to detect pathological alterations in cardiac tissue using an Eclipse Ci-L microscope.

**Masson's staining:** Images of tissue regions of interest were captured at 200X magnification using an Eclipse Ci-L microscope. Post-imaging, the Image-ProPlus 6.0 program facilitated the standardization of measurements in terms of pixel area. Collagen pixel area, collagen Integrated Optical Density (IOD), and corresponding tissue pixel area were measured in three fields per slide. The proportion of the positive area (%) was determined by dividing the area of collagen pixels by the area of tissue pixels, multiplied by 100.

**RT-PCR detection of inflammation-related gene protein expression:**

Using the TRizol technique, complete RNA was isolated from the sinoatrial node tissues of the trio of mouse groups. The process of reverse transcription and RT-PCR adhered to the guidelines provided in the kit.

**Conditions for reverse transcription:** 25° for 5 min, 42° for 30 min, and 85° for 5 s.

**Conditions for RT-PCR reaction:** Start at 95° for

30 s, then proceed with 40 sequences of 95° for a 15 s and 60° for 30 s. Melting curve analysis was conducted from 65° to 95° with a 0.5° increment, capturing fluorescence signals at each step.

GSDMD served as the internal benchmark gene, with the comparative expression rates of target genes in each cluster determined through the $2^{-\Delta\Delta Ct}$ technique. Table 1, elaborates on the sequences of primers for every gene targeted.

**TABLE 1: PRIMER SEQUENCES FOR QUANTITATIVE PCR**

| Primer name | Primer sequence (5'-3') |
|---|---|
| GAPDH | Forward: CCTCGTCCCGTAGACAAAATG |
| GAPDH | Reverse: TGAGGTCAATGAAGGGGTCGT |
| NLRP3 | Forward: TAAGAACTGTCATAGGGTCAAAACG |
| NLRP3 | Reverse: GTCTGGAAGAACAGGCAACATG |
| CASP1 | Forward: TTGAAAGACAAGCCCAAGGTG |
| CASP1 | Reverse: CCAAGTCACAAGACCAGGCATA |
| IL-1β | Forward: AGGCTCCGAGATGAACAACAAA |
| IL-1β | Reverse: GTGCCGTCTTTCATTACACAGGA |
| IL-18 | Forward: AGACCTGGAATCAGACAACTTTGG |
| IL-18 | Reverse: GGGTCACAGCCAGTCCTCTT |
| GSDMD | Forward: GAGCTTTATGCTTGAAGGGTGA |
| GSDMD | Reverse: ATGGAACAAAGCGCAGCAA |

**Statistical methods:**

The analysis of the experimental data was conducted utilizing Statistical Package for the Social Sciences (SPSS) 19.0 software along with Image-Pro Plus. The data is displayed as an average plus or minus the standard deviation ($\bar{x}\pm s$). To analyze quantitative data, a one-way Analysis of Variance (ANOVA) was employed to evaluate group variances, succeeded by Lysergic Acid Diethylamide (LSD) or Dunnett T3 post-hoc tests to compare any two groups. All statistical evaluations employed a significance threshold of Alpha ($\alpha$)=0.05. A $p<0.05$ was deemed to hold statistical significance.

## RESULTS AND DISCUSSION

By employing the TCMSP and BATMAN-TCM systems, a screening was conducted on 127 possible active components of YXFMs. TCMSP specifically pinpointed 59 substances in *Salvia miltiorrhiza*, 17 in *Astragalus membranaceus*, 6 in *Ligusticum chuanxiong*, 17 in *Panax ginseng*, alongside 9 derived from *Schisandra chinensis*, whereas BATMAN-TCM pinpointed 19 different substances from *O. japonicus*. The effective ingredients were listed in Table 2. Following the prediction of their targets and elimination of duplicates, a sum of 453 distinct targets were identified.

Using the search terms SSS data were searched in GeneCards, OMIM, and DisGeNET databases. After removing duplicates, 882 disease targets related to SSS were identified.

The Venny platform was utilized to examine the intersecting targets of YXFMs active ingredients and SSS disease targets. The drug gene count was 453, the disease gene count was 882, and the intersection gene count between drug and disease was 129 (fig. 1). Key components of YXFMs were pinpointed, leading to the creation of a drug-ingredient-target network model utilizing Cytoscape 3.7.2 software (fig. 2), comprising 300 nodes and 928 edges. The top 7 compounds identified were quercetin, stigma sterol, luteolin, kaempferol, guanosine, tanshinone IIA, and beta-sitosterol.

**TABLE 2: ACTIVE INGREDIENTS OF YXFMs**

| Molecule name | Score | Drug |
|---|---|---|
| Ophiopogonone B | 48 | *O. japonicus* |
| Ophiopogonin A | 48 | *O. japonicus* |
| Uridine | 122.778 | *O. japonicus* |
| Ophiopogonone A | 15.365 | *O. japonicus* |
| 6-aldehydo-isoophipogonone B | 48 | *O. japonicus* |
| Ophiopogonanone A | 48 | *O. japonicus* |
| Methyl ophi opogonanone B | 80.882 | *O. japonicus* |
| Guanosine | 122.778 | *O. japonicus* |
| Ophiopogonin C | 48 | *O. japonicus* |
| Methyl ophiopogonanone A | 48 | *O. japonicus* |
| Ophiopogonanone C | 48 | *O. japonicus* |

| | | |
|---|---|---|
| Ophiopogonanone E | 80.882 | *O. japonicus* |
| N-trans-feruloyltyramine | 48 | *O. japonicus* |
| Ophiopogonin D | 48 | *O. japonicus* |
| Ophiopogonin B | 48 | *O. japonicus* |
| Stigmasterol | 80.882 | *O. japonicus* |
| Ophiopogon B | 48 | *O. japonicus* |
| Ophiopogon A | 48 | *O. japonicus* |
| Orchinol | 80.882 | *O. japonicus* |

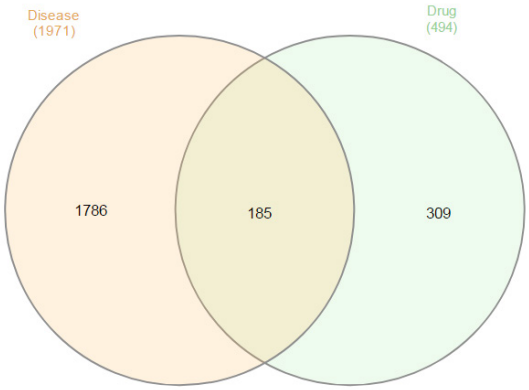


**Fig. 1: Venn diagram of YXFMs components and SSS targets**

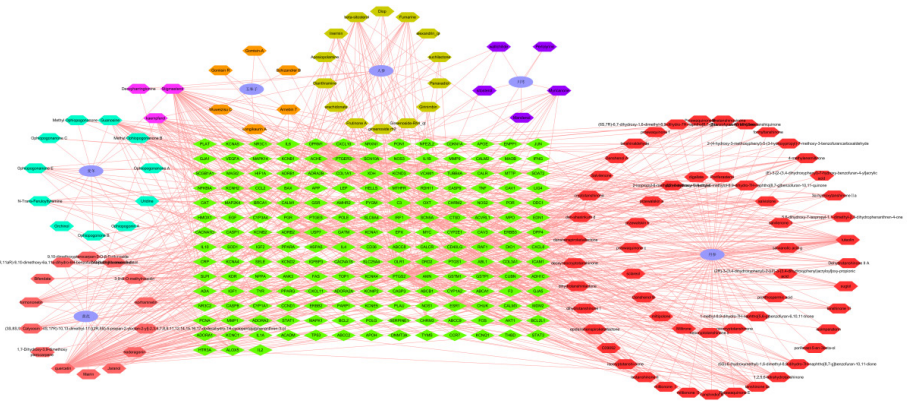

**Fig. 2: Drug-ingredient-target network model**

The collective target data of YXFMs and SSS were inputted into the STRING database for establishing PPI network links, with a foundational interaction score of 0.4 and the exclusion of isolated nodes. Using Cytoscape 3.7.2 software, the PPI data was moved to construct the PPI network (fig. 3). Nodes with brighter colors and larger sizes indicate higher degree values, suggesting their greater importance in the network. Using R software, the connectivity nodes of core genes were determined and a bar graph of the top 30 core genes was generated (fig. 4). The core genes include Tumor Necrosis Factor (TNF), AKT Serine/Threonine Kinase 1 (AKT1), IL6, Tumor Protein P53 (TP53), IL-1β, Vascular Endothelial Growth Factor A (VEGFA), CASP3, JUN, Matrix Metallopeptidase 9 (MMP9), and Prostaglandin-Endoperoxide Synthase 2 (PTGS2).

Using R software and its underlying database org. Hs.eg.db, gene IDs (entrezID) of potential target genes were obtained. Subsequently, bioconductor was employed to conduct GO functional enrichment analysis on these prospective target genes. Each category was ranked based on significance, and the top 10 enriched terms were visualized in the form of a bar graph (fig. 5), where the length of the bars represents the number of genes enriched in GO terms, and colors indicate the significance of enrichment. Findings suggest that YXFMs play

a role in biological functions, mainly in reacting to lipopolysaccharide and bacterial-derived molecules, reaction to metal ions, control of blood flow, and reaction to antibiotics.

Subsequently, bioconductor facilitated the execution of KEGG pathway enrichment studies on these prospective target genes, establishing a significance level at $p \leq 0.05$. The top 20 enriched pathways were ranked based on significance and visualized in the form of a bubble chart (fig. 6). Findings show that YXFMs mainly target lipid and atherosclerosis, as well as fluid shear stress and atherosclerosis in treating SSS. Pathways involve TNF, C-type lectin receptor, and IL-17 signaling. It is speculated that the active ingredients of YXFMs may target multiple signaling pathways to treat SSS.

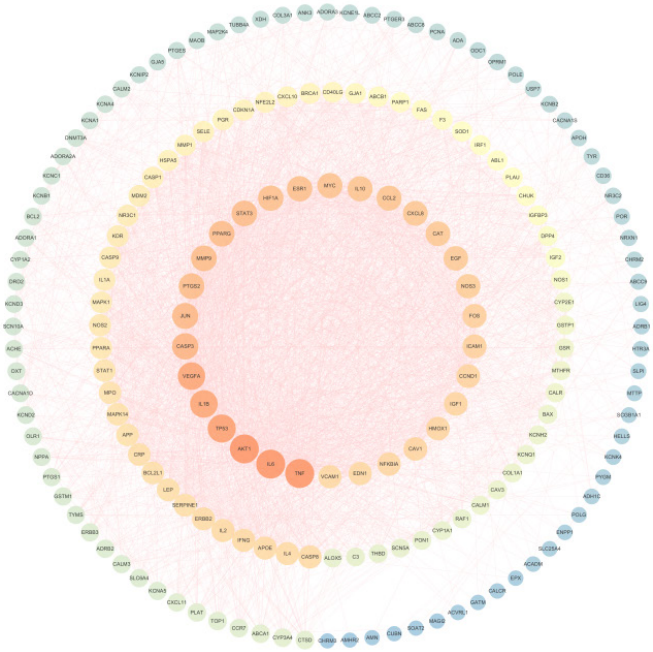

**Fig. 3: PPI network of YXFMs and SSS**

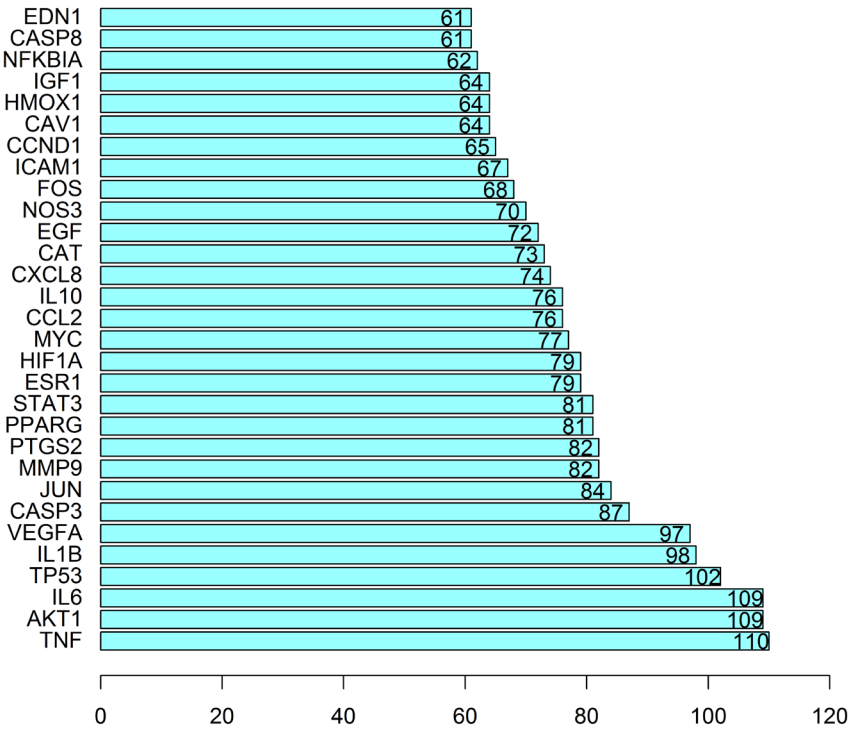


**Fig. 4: Bar graph of the top 30 core genes**

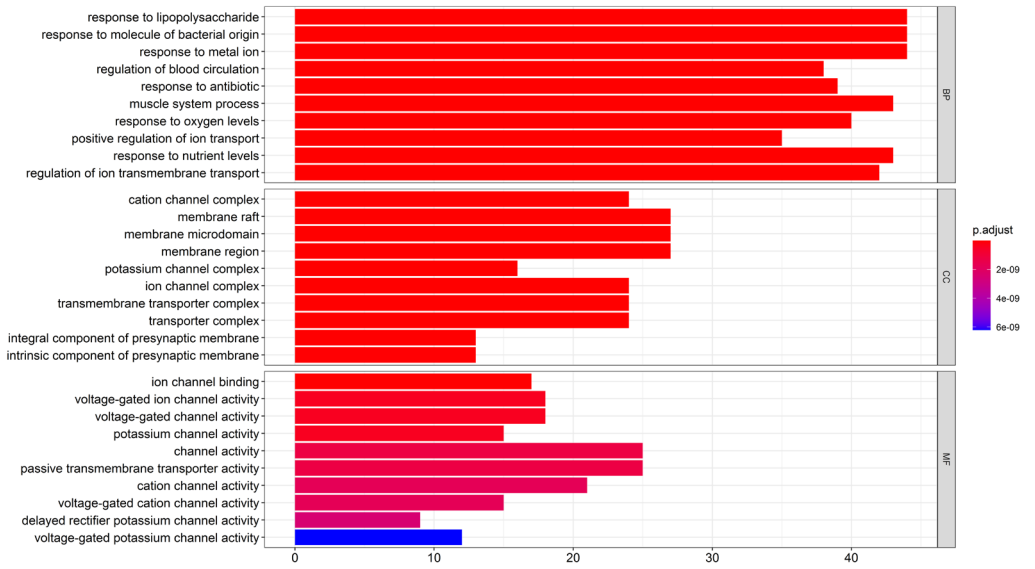


**Fig. 5: GO enrichment analysis of YXFMs**

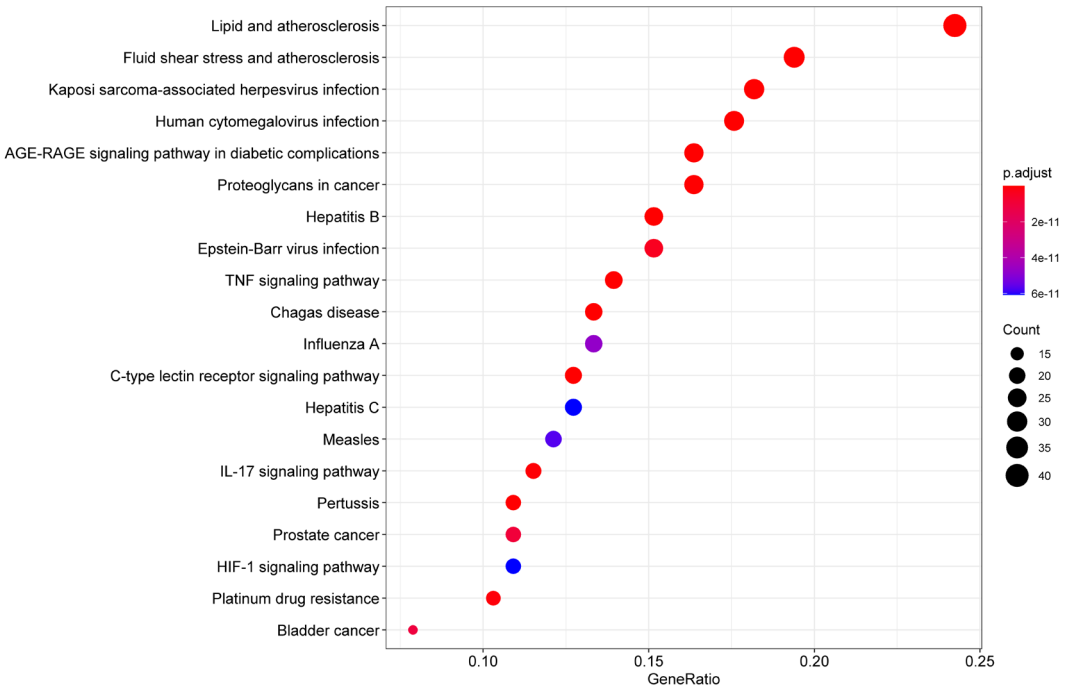


**Fig. 6: KEGG enrichment analysis of YXFMs**

The core active ingredients of YXFMs in treating SSS include quercetin, stigma sterol, luteolin, kaempferol, guanosine, tanshinone IIA, and beta-sitosterol. The primary targets of YXFMs in treating SSS are TNF, AKT1, IL6, TP53, IL1B, among others (Table 3). Investigating the KEGG pathway uncovered that these genes affect heart rate, possibly through routes associated with lipid and atherosclerosis, fluid shear stress and atherosclerosis, the Receptor for Advanced Glycation Endproducts (RAGE) signaling pathway in diabetes, and the TNF signaling pathway methods involving C-type lectin receptor, IL-17, and Hypoxia-Inducible Factor (HIF)-1. Utilizing Cytoscape 3.7.2 software, a graphical representation of drug active ingredients-disease targets-signaling pathways was developed for YXFMs addressing SSS (fig. 7). Using the built-in network analyzer in this software, the network topology parameters of YXFMs treating SSS were analyzed to identify core components and core target points.

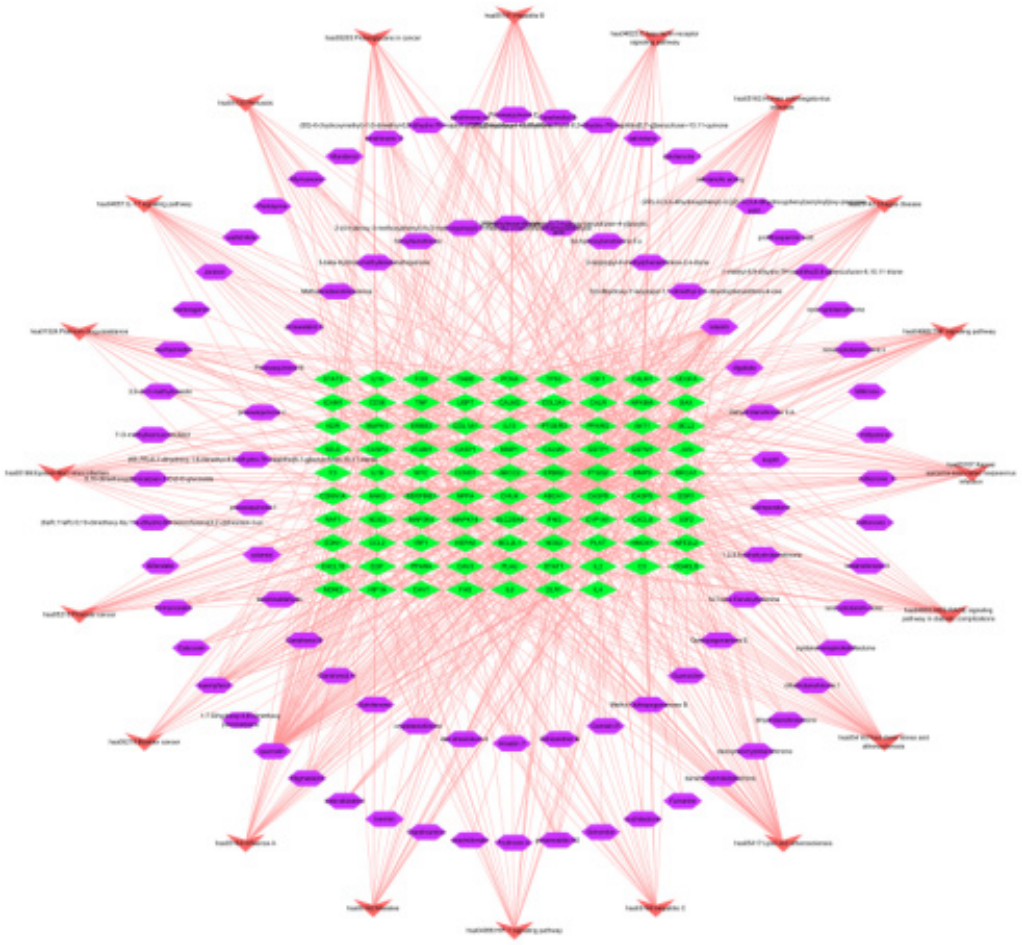

**Fig. 7: Network graph of YXFMs active ingredients-SSS targets-pathways**
**Note: Purple hexagon nodes represent the active ingredients of YXFMs, light green diamonds represent the target genes of active ingredients and red inverted triangles represent the signaling pathways influenced by active ingredients**

The mice in the normal group exhibited good health status with normal diet and stool, black shiny fur, smooth and glossy coat, and no deaths occurred. In the control group, mice showed signs of depression with reduced food intake, greyish-white fur lacking luster, and one death occurred during the experiment period. The QXN group showed improvements compared to the model group, with normal food intake and noticeable improvement in fur color compared to the model group, and no deaths occurred.

The functionality of the SAN in mice was assessed through electrocardiography techniques and Masson staining. Heart rate readings from the electrocardiogram revealed a notable decrease in SSS mice relative to the control group, in contrast to the YXFMs group where there was a marked enhancement in heart rate (fig. 8). Masson staining results showed a significantly higher degree of fibrosis in the SAN of the SSS group compared to the control group, and a more pronounced fibrosis in the YXFMs group than in the SSS group. This indicates that YXFMs markedly enhanced SAN functionality and mitigated SAN fibrosis caused by aging.

After 8 w, the echocardiographic examination of mice from both cohorts showed significant changes compared to the control group; within the model group, there was a substantial reduction in LVPWs and LVPWd ($p<0.01$, $p<0.05$), whereas there was a significant rise in LVIDs and LVIDd ($p<0.01$). In the case of FS, there was a notable reduction in EF ($p<0.01$), accompanied by a marked decrease in heart rate ($p<0.05$). Compared to the model group, the QXN group showed significant increases in EF, FS ($p<0.01$, $p<0.05$), and a faster heart rate ($p<0.01$, $p<0.05$), with decreases in LVIDs, LVIDd ($p<0.01$, $p<0.05$), and increases in LVPWs, LVPWd ($p<0.01$, $p<0.05$) as shown in Table 3 and fig. 9.

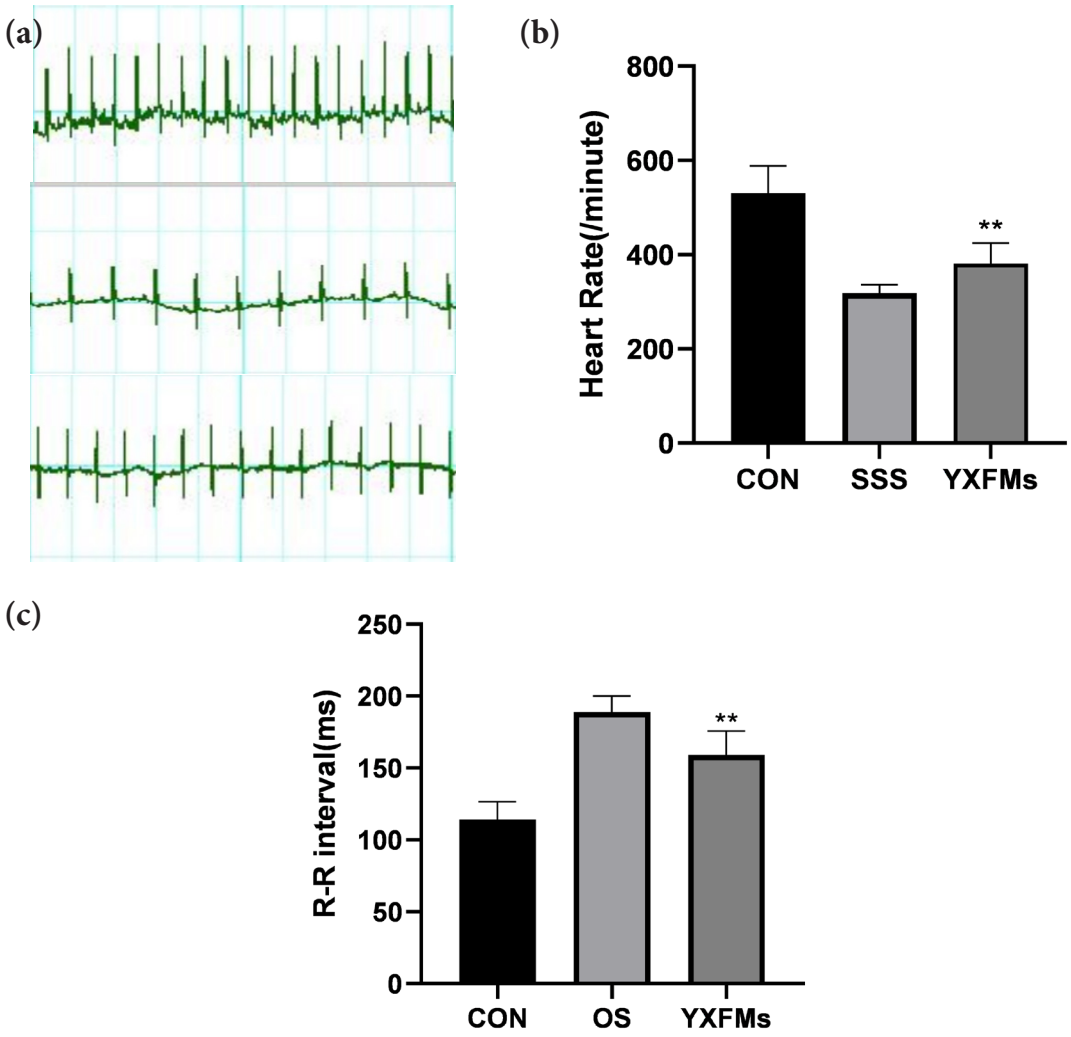


**Fig. 8: YXFMs improve SAN function and increase heart rate in SSS mice, (a): Resting heart rate of mice in each group (125 ms/division); (b): Statistical analysis of heart rate in each group and (c): Statistical analysis of R-R interval**
**Note: **p<0.01**

**TABLE 3: VENTRICULAR STRUCTURE AND FUNCTIONAL PARAMETERS OF MICE IN EACH GROUP (x̄±s)**

| Group | LVIDs/mm | LVIDd/mm | LVPWs/mm | LVPWd/mm | EF/ % | FS/ % |
|---|---|---|---|---|---|---|
| Control | 1.80347 | 2.64282 | 1.23634 | 0.95278 | 61.8768 | 31.7597 |
| Model | 2.93773 | 3.95857 | 1.16829 | 0.87338 | 51.3116 | 25.788 |
| QXN | 2.69954 | 3.8338 | 1.10023 | 0.93009 | 57.3221 | 29.5858 |

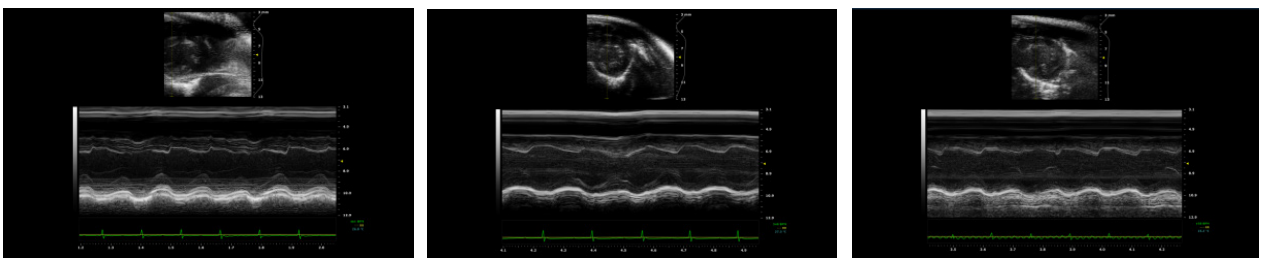

Control group Model group QXN group

**Fig. 9: Echocardiographic results of mice in each group**

The outcomes of H&E staining revealed clear structures of the endocardium, myocardium, and epicardium in the control group, without notable atypical alterations in the heart wall or cavity. Myocardial fibers were stained uniformly, cell boundaries were clear, cells were evenly distributed, striations of myocardial cells were distinct, and no abnormal interstitial changes or inflammatory alterations were observed. In the model group, H&E staining of mouse heart tissues revealed hypertrophy of myocardial cells, increased interstitial components, and deposition of insoluble fibrin proteins in the endocardium, myocardium, and epicardium. There was also noticeable inflammation infiltration. In the YXFMs group, HE staining of mouse heart tissues showed some improvement in myocardial fiber inflammation, with reduced inflammation infiltration compared to the model group as shown in fig. 10.

Masson staining results showed that in the control group, myocardial cell morphology was normal without significant collagen deposition. In the model group, Masson staining of mouse heart tissues revealed extensive collagen fiber deposition in the intercellular spaces. In the QXN group, Masson staining showed a significant reduction in collagen fibers in the intercellular spaces of myocardial tissues. There was a notable increase in the Collagen Volume Fraction (CVF) in the model group compared to the control group ($p<0.01$); CVF in the QXN group decreased compared to the model group ($p<0.01$ and $p<0.05$), indicating that QXN can significantly reduce myocardial fibrosis induced by D-galactose aging in mice as shown on fig. 11.

Fig. 6, illustrates a notable increase in messenger RNA (mRNA) concentrations of NLRP3, CASP1, GSDMD, IL-1β, and IL-18 in the model group, in contrast to the control group ($p<0.01$). Following administration of QXN, mRNA levels of NLRP3, CASP1, GSDMD, IL-1β, and IL-18 showed varying degrees of reduction ($p<0.01$ and $p<0.05$), as depicted in fig. 12.

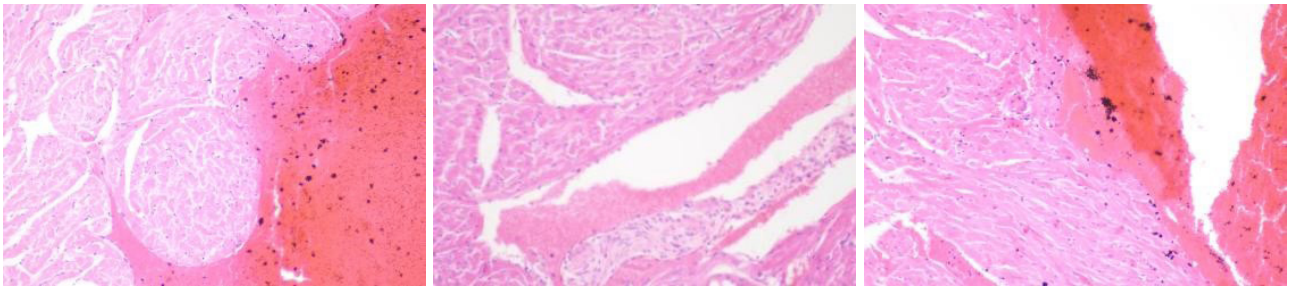

Control Group Model Group YXFMs Group

**Fig. 10: Morphology of sinus node tissue by H&E staining (200X)**

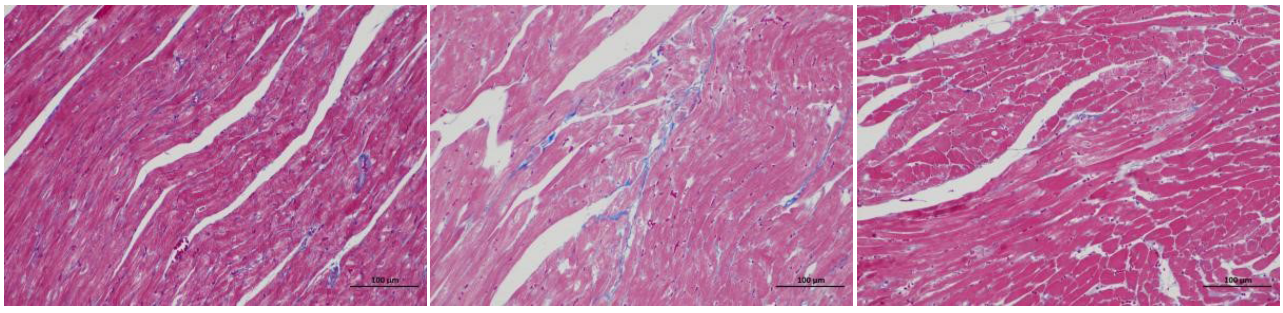

Control Group Model Group YXFMs Group

**Fig. 11: Myocardial tissue morphology by Masson staining (200X)**

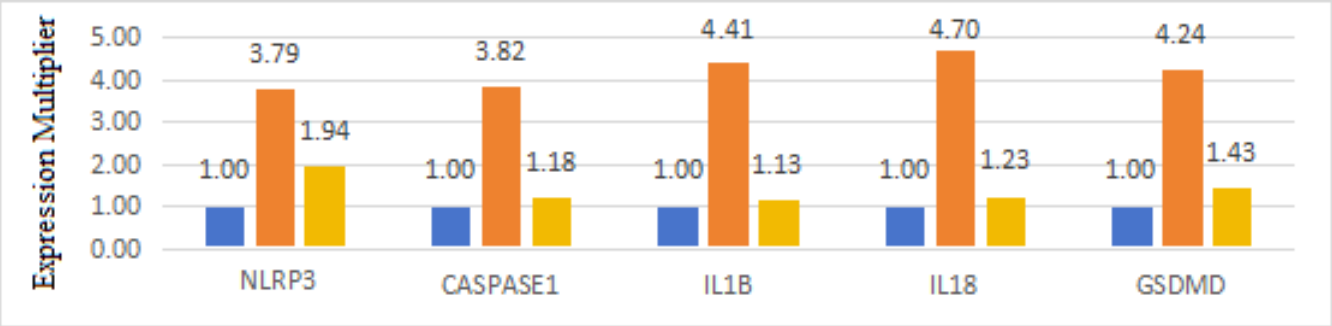


**Fig. 12: Differential mRNA expression in sinus node tissues**
**Note: (■): Control group; (■): Model group and (■): QXN group**

TCM has shown significant efficacy in treating SSS[5]. YXFMs are commonly used in clinical practice for treating chronic arrhythmias of qi-yin deficiency type. Previous animal experiments have demonstrated that YXFMs improve sinus node fibrosis in mice. Zhang *et al*.[6] discovered that in live experiments, YXFMs markedly reduced age-related SSS, decreased the R-R interval, heightened heart rate, and enhanced sinus node fibrosis in mice with SSS. *In vitro* experiments showed that YXFMs effectively suppressed Hydrogen peroxide ($H_2O_2$)-induced oxidative damage in cells, promoted Nuclear factor erythroid 2-related factor 2 (Nrf-2) activation and nuclear translocation, increased Heme Oxygenase-1 (HO-1) expression to inhibit Reactive Oxygen Species (ROS) proliferation, and ultimately upregulated Hyperpolarization activated Cyclic Nucleotide gated potassium channel 4 (HCN4) expression by inhibiting Histone Deacetylase 4 (HDAC4). Apart from improving sinus node function, YXFMs also affect the nervous system. Li *et al*.[7] found that while improving mouse heart rate, YXFMs promoted the expression of Peroxisome proliferator-activated receptor Gamma Coactivator 1-Alpha (PGC-1α) and Nrf-2 proteins, thereby ameliorating pathological damage related to brain tissue and further reducing neuronal apoptosis. Clinical studies have demonstrated the efficacy of YXFMs in treating chronic arrhythmias. Zhang *et al*.[8] found that YXFMs effectively treated chronic arrhythmias of qi-yin deficiency and blood stasis type, significantly increasing average heart rate, minimum heart rate, and total beats, improving clinical symptoms with good safety. Clinical research showed that YXFMs significantly reduced premature ventricular contractions in children[9], demonstrating a bidirectional regulatory effect on arrhythmias. Based on the clinical efficacy of YXFMs and previous animal studies, we chose YXFMs to explore their therapeutic mechanisms in treating SSS.

Currently, the issue of aging population is increasingly severe, prompting continuous research into mechanisms to delay aging and the establishment of aging models. Researchers have selected various animal aging models, among which the D-galactose induced subacute aging model is the most widely used[10]. In this study, mice were injected subcutaneously in the neck and back with D-galactose (200 mg/kg/d) continuously for 8 w. In contrast to the control group, the mice exhibited suboptimal health, indicated by lower levels of LVPWs and LVPWd, heightened occurrences of LVIDs and LVIDd, a notable reduction in FS and EF, a decelerated heart rate, and pronounced histopathological alterations in cardiac ultrasonography. This suggesting heart malfunctions and changes in the ventricles of elderly mice, thereby validating the effective modeling.

Through network pharmacology analysis, we found that various inflammatory factors play a role in the treatment of SSS by YXFMs. Experimental findings revealed that the mice in the model group, in contrast to the control group, displayed subpar mental health, notably grayish-white fur, and heightened inflammatory indicators. Post the gastric infusion of YXFMs, the psychological condition of the mice showed improvement, their fur condition markedly surpassed the model groups, and there was a notable enhancement in the histopathological damage to the sinus node tissue. Moreover, there was a significant decrease in mRNA expression levels of NLRP3, CASP3, GSDMD, IL-1β, and IL-18, indicating that YXFMs can ameliorate inflammatory infiltration

and fibrosis of the sinus node cells in D-galactose induced aging mice.

The research utilized network pharmacology techniques to investigate YXFMs roles in managing SSS, verifying YXFMs therapeutic impact through the regulation of various targets and pathways, including substance metabolism, The process of transmitting signals, along with the inflammatory reaction. This lays a solid foundation for further research and validation of its mechanisms in clinical applications and scientific studies. However, many disease-related targets and pathways require further experimental verification.

**Acknowledgments:**

This work was supported by grants from the National Natural Science Foundation (No: 81874403) and Foundation of Liaoning Xingliaoyingcai Plan (No: XLYC1802099).

**Conflict of interests:**

The authors declared no conflict of interests.

## REFERENCES

1. Heart Disease and Stroke Statistics-2017 Update: A report from the American heart association. Circulation 2017;136:e196.
2. Ru J, Li P, Wang J, Zhou W, Li B, Huang C, *et al*. TCMSP: A database of systems pharmacology for drug discovery from herbal medicines. J Cheminform 2014;6:1-3.
3. Liu Z, Guo F, Wang Y, Li C, Zhang X, Li H, *et al*. BATMAN-TCM: A bioinformatics analysis tool for molecular mechanism of traditional Chinese medicine. Sci Rep 2016;6(1):21146.
4. Szklarczyk D, Gable AL, Lyon D, Junge A, Wyder S, Huerta-Cepas J, *et al*. STRING v11: Protein-protein association networks with increased coverage, supporting functional discovery in genome-wide experimental datasets. Nucl Acids Res 2019;47(D1):D607-13.
5. Zheng YP, Gong KM, Yao XY, Chai X, Fan L, Wang H. Clinical observation on treatment of bradyarrhythmia with Chinese herbal medicine. J Tradit Chin Med 1993;13(3):163-8.
6. Zhang H, Li L, Hao M, Chen K, Lu Y, Qi J, *et al*. Yixin-Fumai granules improve sick sinus syndrome in aging mice through Nrf-2/HO-1 pathway: A new target for sick sinus syndrome. J Ethnopharmacol 2021;277:114254.
7. Li YZ, Deng J, Zhang XD, Li DY, Su LX, Li S, *et al*. Naringenin enhances the efficacy of ferroptosis inducers by attenuating aerobic glycolysis by activating the AMPK-PGC1α signalling axis in liver cancer. Heliyon 2024.
8. Zhang H, Chen C, Liu Y, Ren L, Qi J, Yang Y, *et al*. NRF-2/HO-1 pathway-mediated SHOX2 activation is a key switch for heart rate acceleration by Yixin-Fumai granules. Oxid Med Cell Longev 2022;2022(1):8488269.
9. Bonnet U. Ten years of maintenance treatment of severe melancholic depression in an adult woman including discontinuation experiences. Fortsch Neurol Psychiatr 2024.
10. Haider S, Liaquat L, Shahzad S, Sadir S, Madiha S, Batool Z, *et al*. A high dose of short term exogenous D-galactose administration in young male rats produces symptoms simulating the natural aging process. Life Sci 2015;124:110-9.